THEORETICAL MODELING AND EXPERIMENTAL ANALYSES OF LAMINATED WOOD COMPOSITE POLES[1]

Cheng Piao

Postdoctoral Research Scientist

Todd F. Shupe†

Associate Professor
School of Renewable Natural Resources
Louisiana State University AgCenter
Baton Rouge, LA 70803

Vijaya Gopu

Professor and Chair
Civil and Environmental Engineering
Tulane University
New Orleans, LA 70118

and

Chung Y. Hse†

Principle Wood Scientist
USDA Forest Service
Southern Research Station
Pineville, LA 71360

(Received April 2003)

ABSTRACT

Wood laminated composite poles consist of trapezoid-shaped wood strips bonded with synthetic resin. The thick-walled hollow poles had adequate strength and stiffness properties and were a promising substitute for solid wood poles. It was necessary to develop theoretical models to facilitate the manufacture and future installation and maintenance of this novel engineered wood product. A higher-order governing differential equation (GDE) model was developed for this purpose based on the principle of minimum potential energy. Transverse shear and glue-line effects were taken into account in the development of the model. A simplified theoretical model was also derived to further validate the higher-order GDE model. Thirty-six small-scale wood laminated composite poles were made and tested to validate the models developed. Strip thickness and number of strips were chosen as experimental variables. The deflection predicted by the theoretical models agreed well with those measured in experiment. The agreement with the results predicted by the simplified theoretical model was better than that with those predicted by the higher-order GDE model.

Keywords: Beams, composites, energy methods, higher-order differential equation, poles, thick-shell, Timoshenko beam theory, variational methods.

INTRODUCTION

Wood laminated composite poles are thick-walled members with a polygonal cross-section. The hollow poles have adequate strength and stiffness properties but are lower in weight, when compared to solid wood poles. The advantages of wood composite poles include: (1) they can be produced from renewable natural resources; (2) they can be made from low quality materials, such as small logs and processing residues; and (3) they can be easily treated.

[1] This paper (No. 03-40-1172) is published with the approval of the Director of the Louisiana Agricultural Experiment Station.

† Member of SWST.

© 2005 by the Society of Wood Science and Technology

These advantages make the hollow pole superior to solid wood poles or poles made from other materials for similar applications. To enhance material and structural efficiencies of these members, theoretical research is needed.

The classical Bernoulli-Euler theory has long been used in structural analysis and design of slender beams. The main assumption in this theory is that transverse plane sections that are normal to the beam middle plane before bending remain plane and normal to beam middle plane after bending. This assumption implies that the transverse shear strain and deformation are negligible. The Bernoulli-Euler theory may lead to serious discrepancies in the case of deep beams with small slender ratios (L/h). Grashof (1878) and Rankine (1895) conducted earlier investigations of the shear effect on the elastic deflection curve of beams. Timoshenko (1921) improved the validity of the Bernoulli-Euler theory by incorporating the effect of transverse shear into the governing equations. The Timoshenko theory assumed that the cross-section remains plane after bending and the shear stress is uniform throughout the thickness of the beam. In order to recognize the nonuniform shear stress distribution at a section, a factor was introduced into the shear stress formula. Numerous other theories have been proposed to include the transverse shear and to improve upon the Timoshenko theory in the last three decades (Rehfield and Murthy 1982; Kant and Gupta 1988; Valisetty 1990; Kathnelson 1996). None of these theories have dealt with thick-walled and polygonal beams. A classical theory of shear stress distribution in a cross-section was developed by Timoshenko (1976). The shear stress distribution can be related to the deformation of a beam and thus can be included in a higher-order governing differential equation, from which the governing equation can be obtained.

One of the earliest studies of shear effects on deflection in wood members was done by Biblis (1965). Two methods were used in his study, i.e., an elementary method and the energy method. In the elementary method, it was assumed that all cross-sections were free to deform and the curve due to shear was represented by two straight lines, whereas the energy method had no such assumptions and was more accurate.

This study deals with development of a higher-order governing differential equation (GDE) model that takes into account the effects of shear. The higher-order GDE was derived based on the principle of minimum potential energy. A simplified beam model was also derived to validate the higher-order GDE model. Energy concepts were also used to derive the simplified model, and a factor was introduced to correct the errors caused by the assumption of uniform-shear.

The objectives of the study were to:

1. Develop a theoretical model to analyze hollow, polygonal-shaped composite poles based on higher-order governing differential equations and the principle of minimum potential energy.
2. Utilize the simplified beam theory to compare the results predicted by the higher-order GDE model.
3. Evaluate effects of glue-lines on the deflection of composite poles.
4. Evaluate transverse shear effects on the deflection of hollow irregular-shaped wood composite poles.

HIGHER-ORDER GOVERNING DIFFERENTIAL EQUATION MODEL

The composite poles (Fig. 1) investigated in this study are composed of a number of wood strips bonded with an adhesive such as resorcinol-phenol-formaldehyde resin. Since the thickness of the strips is less than the outer radius of the circle enclosing the cross-section, the poles are hollow inside. Figure 1 shows a typical geometry and lay-up of a polygonal wood composite pole and its right-hand set of coordinate axes x, y, and z. The corresponding axial displacements are u, v, and w.

The lateral displacement (w) of the pole was assumed to consist of four parts: bending and shear deformations of the wood strips and glue layers. In this study, the normal and shear strain energies for wood and glue layers were derived.

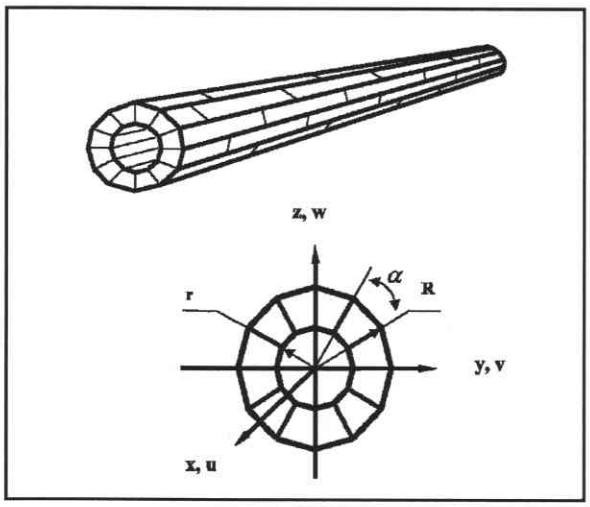

FIG. 1. A schematic diagram of a wood composite pole and its coordinates.

Since the thickness of each glue layer is much thinner than that of a wood strip, glue layer thickness was neglected in the analysis of strain energy of wood strips. Strain energy stored in glue layers was analyzed separately from wood strips.

The normal stress in the pole can be expressed as

$$\sigma_x = \frac{Mz}{I} \tag{1}$$

where M is bending moment, z the z coordinate, and I is the moment of inertia of the cross-section of the pole with respect to the y axis. The shear stress is given as

$$\tau_{xy} = \frac{dM}{dx}\frac{1}{bI}\int_z^R z dA = \frac{VQ}{Ib} \tag{2}$$

where V is the vertical shear force, b the width of the wood shell measured at z and parallel to the y axis, Q the first moment of the pole cross-section, and R the radius of the enclosing circle of the pole. Equation (2) can be used to calculate the shear strain energy of the pole and included in the higher-order differential equation by relating the shear stress distribution to the deformation of a beam. The normal and shear strain energy density functions for a beam are first calculated. In the Cartesian coordinate system, they are defined as (elementary mechanics)

$$W_\sigma = \frac{1}{2}\sigma_x \varepsilon_x \tag{3}$$

$$W_\tau = \frac{1}{2}\tau_{xy}\gamma_{xy} \tag{4}$$

where ε_x is the normal strain and γ_{xy} the shear strain. They are expressed as follows:

$$\varepsilon_x = \frac{du_x}{dx} = -z\frac{d^2w}{dx^2} \tag{5}$$

$$\gamma_{xy} = \frac{\tau_{xy}}{G} \tag{6}$$

where G is the modulus of rigidity of wood (764.8 MPa (0.11 Mpsi) (Bodig and Jayne (1982))). Thus, the strain energy functions become

$$W_\sigma = \frac{1}{2}\sigma_x\varepsilon_x = \frac{1}{2}E\varepsilon_x^2 = \frac{1}{2}E\left(\frac{d^2w}{dx^2}\right)^2 z^2 \tag{7}$$

$$W_\tau = \frac{1}{2}\tau_{xy}\gamma_{xy} = \frac{1}{2}\frac{\tau_{xy}^2}{G} = \frac{1}{2}\frac{V^2Q^2}{GI^2b^2} \tag{8}$$

where E is the Young's modulus of the wood. E values were determined in an experimental study of the composite poles. Equation (8) is still a formula, which can be transformed and related to the deformation of the poles. Substituting $V = -EI(d^3w/dx^3)$ in Eq. (8) we have

$$W_\tau = \frac{1}{2}\frac{V^2Q^2}{GI^2b^2} = \frac{1}{2}\frac{E^2Q^2}{Gb^2}\left(\frac{d^3w}{dx^3}\right)^2 \tag{9}$$

After integrating Eqs. (7) and (9) with respect to y and z and substituting the value of I, the normal strain energy and shear strain energy of the wood would be as follows:

$$U_\sigma = \frac{EI}{2}\int_0^L \left(\frac{d^2w}{dx^2}\right)^2 dx \tag{10}$$

$$U_\tau = \frac{E^2}{2G}\int_0^L \left(\frac{d^3w}{dx^3}\right)^2 dx \int_A \frac{Q^2}{b^2} dydz \tag{11}$$

Let $k_1 = \int_A (Q^2/b^2)dydz$ and substitute it in Eq. (11), then shear strain energy for the wood in the pole has the form

$$U_\tau = \frac{k_1 E^2}{2G} \int_0^L \left(\frac{d^3w}{dx^3}\right)^2 dx \qquad (12)$$

In this study, the pole has 3n (n = 1, 2, 3, . . .) strips, and thus 3n glue layers. The integer n is an arbitrary number and chosen based on available raw materials, pole sizes, and esthetic requirements. Take the 12-strip pole (n = 4) as an example, it has 12 strips and glue layers, as shown in Fig. 2. The strain energy of each glue layer is the sum of strain energy caused by normal and shear strains. The total strain energy of the glue layers is the sum of the strain energy for each glue layer:

$$U_g = U_{\sigma-AA'} + U_{\tau-AA'} + U_{\sigma-BB'} + U_{\tau-BB'} + \cdots + U_{\sigma-LL'} + U_{\tau-LL'} = U_{AA'} + U_{BB'} + \cdots + U_{LL'}.$$

where $U_{\sigma-AA'}$, $U_{\tau-AA'}$, . . . are the normal strain energy of glue-line AA', shear strain energy of AA', etc., and $U_{AA'}$, $U_{BB'}$, . . . are the sum of normal and shear strain energy of AA', the sum of normal and shear strain energy of BB', etc. Since some of them are equal, the total strain energy of the glue layers can be expressed as

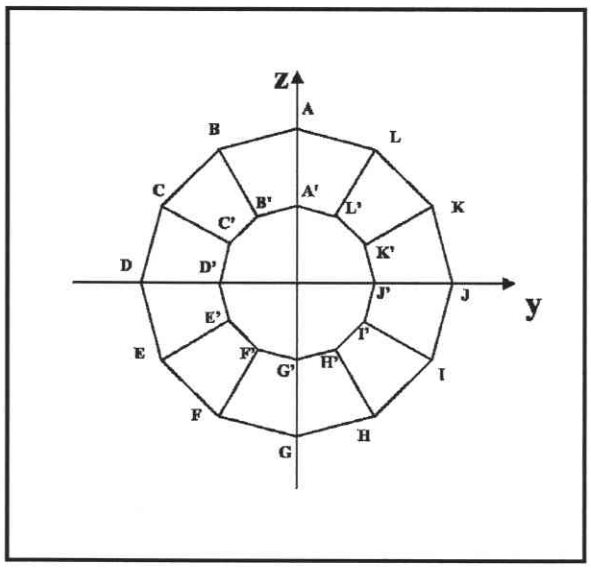

FIG. 2. A schematic diagram of the cross section of a 12-strip pole shell.

$$U_g = 2U_{AA'} + 4U_{BB'} + 4U_{CC'} + 2U_{DD'} = k_6 \int_0^L \left(\frac{d^2w}{dx^2}\right)^2 dx + k_7 \int_0^L \left(\frac{d^3w}{dx^3}\right)^2 dx \qquad (13)$$

where

$$k_6 = E_g(I_{g1} + 2I_{g2} + 2I_{g3})$$
$$k_7 = k_5(k_1 + k_2 + k_3 + k_4)$$
$$k_5 = \frac{E_g^2}{2G_g}$$
$$k_4 = 2\int\int_A \frac{Q_{g1}^2}{t^2 I_{g1}} dA$$
$$k_3 = 4\int\int_A \frac{Q_{g2}^2}{t^2 I_{g2}} dA$$
$$k_2 = 4\int\int_A \frac{Q_{g3}^2}{t^2 I_{g3}} dA$$
$$k_1 = 2\int\int_A \frac{Q_{g4}^2}{t^2 I_{g4}} dA$$

and I_{g1}, I_{g2}, and I_{g3} are the moment of inertia of glue layers, Q_{g1}, Q_{g2}, Q_{g3}, and Q_{g4} are the first moment of each of the glue lines, E_g is the Young's modulus of glue (approximated at 38.6 TPa (5.6 Mpsi)), G_g is the modulus of rigidity of glue (approximated at 2.1 TPa (0.31 Mpsi)), A is the area of the glue-layer cross-section, and t is the thickness of the glue layers.

The two external forces applied to the pole system were body force of pole (p_0) and the applied concentrated load (P) at the free end (Fig. 3). The work done by the external force is as follows:

$$H = -\int_0^L p_0 w dx - Pw(L) \qquad (14)$$

where

H = work done by the external force
p_0 = body force of the pole
w = transverse displacement along the length of the pole L
$w(L)$ = transverse displacement at point L at the end of the pole

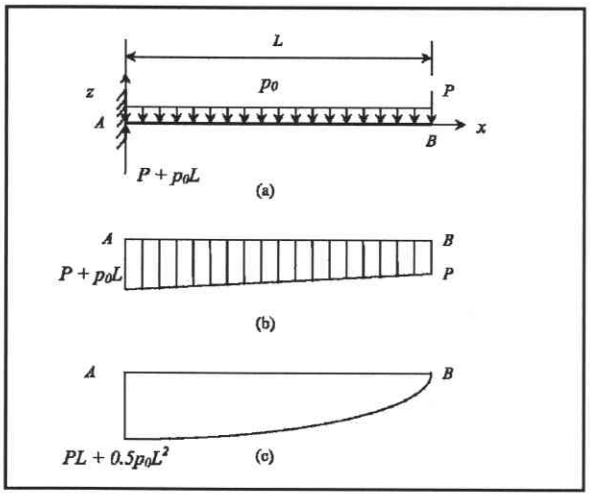

FIG. 3. The loading system and shear and moment distribution of a cantilever beam.

The total potential energy is given as

$$\pi = U_\sigma + U_\tau + U_g + H \tag{15}$$

Substituting Eqs. (10), (12), (13), and (14) into Eq. (15) and rearranging, the total potential energy is given by

$$\pi = k_8 \int_0^L \left(\frac{d^2w}{dx^2}\right)^2 dx + k_9 \int_0^L \left(\frac{d^3w}{dx^3}\right)^2 dx - \int_0^L p_0 w dx - Pw(L) \tag{16}$$

where

$$k_8 = \frac{1}{2} EI + k_6$$

$$k_9 = \frac{k_1 E^2}{2G} + k_7$$

The principle of minimum potential energy states that "of all the displacements which satisfy the boundary conditions of a structural system, those corresponding to stable equilibrium configurations make the total potential energy a relative minimum." According to this principle, the system is in equilibrium when the first variation in π vanishes. Thus the equilibrium condition is

$$\delta\pi = \frac{\partial \pi}{\partial x} dx = 0$$

or

$$k_8 \int_0^L 2 \frac{d^2w}{dx^2} \delta\left(\frac{d^2w}{dx^2}\right) dx + k_9 \int_0^L 2 \frac{d^3w}{dx^3} \delta \left(\frac{d^3w}{dx^3}\right) dx - \int_0^L p_0 \delta w dx - P\delta w(L) = 0 \tag{17}$$

Equation (17) yields one 6th-order differential equation, which is the governing differential equation for the pole loading system.

$$k_9 \frac{d^6w}{dx^6} + k_8 \frac{d^4w}{dx^4} - \frac{p_0}{2} = 0 \tag{18}$$

with boundary conditions

$$\left(k_9 \frac{d^5w}{dx^5} - k_8 \frac{d^3w}{dx^3}\right)\Bigg|_{x=L} = \frac{P}{2} \tag{19}$$

$$\left(k_8 \frac{d^2w}{dx^2} - k_9 \frac{d^4w}{dx^4}\right)\Bigg|_{x=L} = 0 \tag{20}$$

$$k_8 \frac{d^3w}{dx^3}\Bigg|_{x=0} = 0 \tag{21}$$

$$w|_{x=0} = 0 \tag{22}$$

$$w'|_{x=0} = 0 \tag{23}$$

$$k_8 \frac{d^2w}{dx^2}\Bigg|_{x=L} = 0 \tag{24}$$

Equation 18 is a non-homogenous higher-order differential equation. Solving Eq. (18) using the boundary conditions, Eqs. (19)–(24), the following solution is obtained

$$w = C_1 + C_2 x + C_3 x^2 + C_4 x^3 + \frac{1}{48k_8} p_0 x^4 + C_5 e^{k_{10}x} + C_6 e^{-k_{10}x} \tag{25}$$

where

$$k_{10} = \sqrt{\frac{k_8}{k_9}}$$

and $C_1 - C_6$ are constants and are given as

$$C_1 = \frac{k_{10}(p_0L + P)\,(e^{k_{10}L} - e^{-k_{10}L}) + 2p_0}{2k_8k_{10}^4(e^{k_{10}L} + e^{-k_{10}L})}$$

$$C_2 = -\frac{p_0L + P}{2k_8k_{10}^2}$$

$$C_3 = \frac{p_0L^2 + 2PL}{8k_8} + \frac{p_0}{2k_8k_{10}^2}$$

$$C_4 = -\frac{p_0L + P}{12k_8}$$

$$C_5 = \frac{k_{10}(p_0L + P)e^{-k_{15}L} - p_0}{2k_8k_{10}^4(e^{k_{10}L} + e^{-k_{10}L})}$$

$$C_6 = -\frac{k_{10}(p_0L + P)e^{-k_{15}L} + p_0}{2k_8k_{10}^4(e^{k_{10}L} + e^{-k_{10}L})}$$

A SIMPLIFIED THEORETICAL MODEL

The displacement in the x, y, and z directions are U, V, and W, respectively. Since U is a function of (x, y, z), we expand U into a Tylor series (Washizu 1968; Kant and Gupta 1988) about $z = 0$:

$$U(x, y, z) = U(x, y, 0) + \left(\frac{\partial U}{\partial z}\right)_{z=0} z + \frac{1}{2!}\left(\frac{\partial^2 U}{\partial z^2}\right)_{z=0} z^2 + \ldots \tag{26}$$

After retaining the first two terms of Eq. (26),

$$\vec{U} = \vec{U}_0 + z\vec{U}_1 \tag{27}$$

where $\vec{U}_1 = u_1\vec{i}_1 + w_1\vec{i}_3$. Equation (27) is an expression that includes the effect of transverse shear deformation. Two assumptions were made: (1) a cross-section perpendicular to undeformed central line remains perpendicular to the deformed locus, and (2) the displacement is small. Then we have

$$U = u + z\,u_1,\ V = 0,\ W = w$$
$$\varepsilon_x = u' + z\,u_1{}',\ \gamma_{xz} = w' + u_1 \tag{28}$$

The total strain energy of the pole may be expressed as

$$\pi = \int\int_V\int (\sigma_x\varepsilon_x + \tau_{xz}\gamma_{xz})dxdydz - \int_0^L p_0 w dx - Pw \tag{29}$$

According to principle of minimum potential energy, the system is in equilibrium when the first variation in π vanishes:

$$\delta\pi = \int\int_V\int (\sigma_x\delta\varepsilon_x + \tau_{xz}\delta\gamma_{xz})dxdydz - \int_0^L p_0\delta w dx - P\delta w = 0 \tag{30}$$

Substituting Eq. (28) into Eq. (30), we obtain the following equation

$$\int_0^L [N\delta u' + M\delta u_1 + Q(\delta w' + \delta u_1) - p_0\delta w]dx - P\delta w = 0 \tag{31}$$

where

$$N = \int_S\int \sigma_x dydz, \quad M = \int_S\int \sigma_x z dydz,$$
$$Q = \int_S\int \tau_{xz} dydz \tag{32a, b, c}$$

N is the axial force, M the bending moment, and Q the shear force. Integrate Eq. (31) and rearrange, and the following Equation can be obtained

$$\int_0^L [N'\delta u - (Q - M')\delta u_1 + (Q' + p_0)\delta w]dx - [N\delta u - (P - Q)\delta w + M\delta u_1]_{x=L} + [N\delta u + Q\delta w + M\delta u_1]_{x=0} = 0 \tag{33}$$

Then the governing differential equations are as follows:

$$Q' = -p_0 \tag{34a}$$

$$M' = Q \tag{34b}$$

$$N' = 0 \tag{34c}$$

and boundary conditions $P = Q|_{x=L}$, also

$$u(0) = w(0) = u_1(0)\big|_{x=0} = 0 \tag{35a}$$

$$M\big|_{x=L} = 0 \tag{35b}$$

Based on these boundary conditions, Eq. (34) can be solved. Substituting Eq. (28) into Eq. (32), we have

$$N = \int_S\int \sigma_x dtdz = E\int_S\int (u' + zu_1')dydz = EAu' \quad (36a)$$

$$M = \int_S\int \sigma_x zdydz = E\int_S\int \varepsilon_x z^2 dydz = EIu_1' \quad (36b)$$

$$Q = \int_S\int \tau_{xz} dydz = E\int_S\int G\gamma_{xz} dydz = Gk(w' + u_1) \quad (36c)$$

where k is a correction factor and determined by the following formula (Shames and Dym 1985):

$$k = \frac{6(1+v)(1+m)^2}{(7+6v)(1+m)+(20+12v)m^2} \quad (37)$$

where $m = D/d$. D is the diameter of enclosing circle of the cylinder, d is the diameter of the inscribe cycle, and v is the Poisson ratio. Substituting Eq. (36) into Eq. (34), we find that no axial loads are applied,

$$EIu_1'' = kGA\,(w' + u_1) \quad (38)$$

$$KGA[w'' + u_1'] = -p_0 \quad (39)$$

Taking derivative of Eq. (38) and substituting Eq. (39), we have

$$EIu_1''' = kGA(w'' + u_1') = -p_0$$

Integrating the above equation three times,

$$EIu = -\frac{1}{6}p_0x^3 + \frac{1}{2}C_1x^2 + C_2x + C_3 \quad (40)$$

where C_1, C_2, C_3 are constants. Solving Eq. (40) by using the boundary conditions Eq. (35), we obtain the deflection function of a cantilever beam subjected to body force and a concentrated load at the free end:

$$w = \frac{p_0}{24EI}x^4 - \frac{P+p_0L}{6EI}x^3 + \left(\frac{2PL+p_0L^2}{4EI} - \frac{p_0}{2kGA}\right)x^2 + \frac{P+p_0L}{kGA}x \quad (41)$$

The maximum deflection is given as

$$w_{\max} = \frac{PL^3}{3EI} + \frac{p_0L^4}{8\,EI} + \frac{PL}{kGA} + \frac{p_0L^2}{2kGA} \quad (42)$$

The first two terms on the right side of Eq. (42) are the bending deflection components, and the last two terms are the shear deflection components of the total deflection. It is also noted that the EI and GA in Eqs. (41) and (42) are for both wood and glue layers. The maximum deflection is the sum of both wood strips and glue layers.

EXPERIMENTAL STUDY

An experimental investigation was conducted on small-scale composite poles to validate the applicability of the theoretical models. The length of the poles was 1.22 m (4 ft) and the diameter was 7.6 cm (3 in.). The species was southern yellow pine (*Pinus*, sp). Strip thickness and number of strips (NOS) were the two variables. Strip thickness levels were 1.0 cm (0.4 in.), 1.5 cm (0.6 in.), 2.0 cm (0.8 in.), and 2.5 cm (1.0 in.), each of which had 6, 9, and 12 strips. Thirty-six small-scale composite poles were made with three replications for each combination of NOS and strip thickness levels. Lumber was first planed to specific thickness and then cut to target size strips using a table saw. Commercially obtained resorcinol-phenol-formaldehyde (RPF) resin was used to bond the strips. The viscosity and specific gravity of RPF were 800 cps and 1.177, respectively. The glue was uniformly hand-spread onto the two lateral surfaces of each strip at 310 g/m^2 (63.3 lbs/1000 ft^2). Poles were pressed in molds for 36 h in an air-conditioned room. Figure 4 shows three small-scale composite poles pressed in steel molds.

A cantilever test was performed on the composite poles using a RIEHLE machine. The updated digital control system of the RIEHLE was connected to a computer. All small-scale composite poles were tested to failure at about 11% moisture content. The load-deflection curve was obtained for each pole tested in bending. These curves were used to compare the results pre-

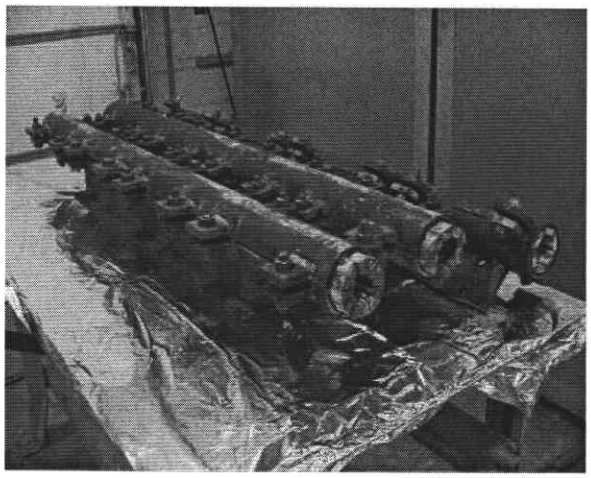

FIG. 4. Small-scale wood composite poles being pressed in steel molds.

dicted by the theoretical models in a specific load range. In the theoretical study, the Young's modulus obtained in the experiment of each pole was used to predict the deformation of the pole. Figure 5 shows a small-scale composite pole being tested in the RIEHLE machine.

RESULTS

Results of theoretical study

The maximum experimental deflections under different loads are compared with those predicted by the theoretical models in Table 1. In

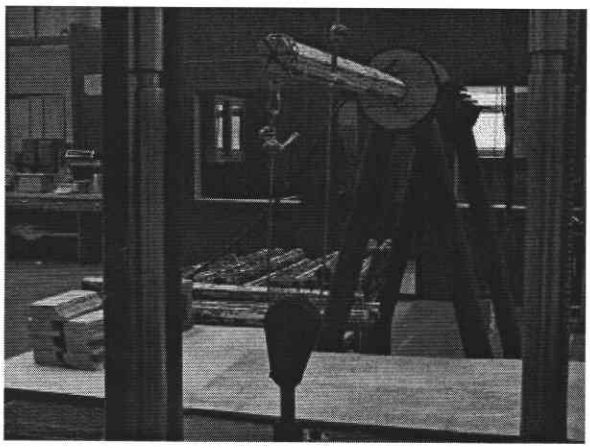

FIG. 5. A small-scale composite pole being tested in a RIEHLE machine.

TABLE 1. *Comparison among the deflection values from experiment and theoretical models of small-scale composite poles with three strip-number levels and four thickness levels.*[1]

Strip number	Strip thickness (cm)	Load (N)	Exp. deflection (cm)	GDE[2] (cm)	Simplified[3] (cm)
12	1.0	178	1.28	1.22	1.28
	1.5	178	1.07	1.00	1.05
	2.0	445	0.92	0.93	0.97
	2.5	445	0.93	0.86	0.90
9	1.0	178	1.92	1.74	1.82
	1.5	178	1.16	1.07	1.11
	2.0	445	1.38	1.31	1.37
	2.5	445	1.09	1.01	1.05
6	1.0	178	1.96	1.85	1.88
	1.5	178	1.94	1.91	1.98
	2.0	445	1.42	1.38	1.41
	2.5	445	1.25	1.23	1.27

[1] Tabled experiment and predicted deflection, and errors are the average of three values.
[2] Higher-order governing differential equation model.
[3] Simplified beam theory model.

this table, each experimental value was the average of three test results. The results predicted by the higher-order GDE model were found to be lower than those predicted by the simplified model. The experimental values were higher than those predicted by the theoretical models.

Table 2 presents the calculated maximum bending stress values based on the elementary mechanics theory and from the higher-order GDE model. Stress values calculated agreed well with those predicted by the models.

The deflections of small-scale composite poles predicted by the higher-order GDE model for different strips and thickness levels are shown in Fig. 6. Figure 6 indicates that the deflection decreased with the increase of strip thickness.

Comparisons were made between results predicted by the higher-order GDE model and the simplified model. Figure 7 shows the results. The values predicted by the two theoretical procedures were very close.

Shear effects on the deflection of small-scale poles were calculated by the simplified beam model and are shown in Fig. 8. Both strip thickness and NOS influence the shear deflection. Shear effects increased with the decrease of strip thickness and with the increase of NOS. Deflec-

TABLE 2. *Comparison between the maximum bending stress values calculated by experimental data and predicted by the higher-order governing differential equation model of small-scale composite poles.*

	Strip thickness (cm)	1.0			1.5			2.0			2.5		
	Sample number	1	2	3	1	2	3	1	2	3	1	2	3
6-strip poles	Theoretical (MPa)	58.71	59.84	58.35	63.61	59.14	74.99	86.16	75.35	70.88	92.05	93.40	93.76
	Experimental (MPa)	60.40	60.79	58.61	61.42	59.72	70.33	85.34	76.26	70.16	92.03	94.70	93.47
9-strip poles	Theoretical (MPa)	48.35	46.73	44.72	64.60	65.69	63.78	69.14	71.62	69.74	86.56	84.86	93.26
	Experimental (MPa)	48.24	46.13	44.91	65.49	67.26	66.49	70.22	67.72	68.57	87.95	84.50	95.37
12-strip poles	Theoretical (MPa)	44.10	33.30	44.30	55.45	44.05	52.09	84.91	75.82	72.93	92.91	69.57	89.78
	Experimental (MPa)	43.00	32.44	43.57	53.78	43.39	49.62	81.53	73.21	69.93	90.62	66.86	85.62

tion due to shear accounted for only 0.8 to 1.9% of the total deflection for the pole tested.

Glue-layer effects on the deflection of composite poles were analyzed by the higher-order GDE model. In the analysis, thickness of the glue layer was set at 0.10 mm (0.004 in.), and Young's modulus and modulus of rigidity of cured resorcinol-phenol-formaldehyde resin were approximated as 38.6 and 2.1 TPa (5.6 and 0.31 Mpsi). The first and second moments, and normal and shear energies of glue lines, were calculated and included in the models. For the small-scale poles, deflection attributed to the glue layers was from 2.3 to 5.5% of the total. No regular patterns were found on the effects of strip thickness and number. These results show that glue-layer effects cannot be neglected. The strong correlation is attributable to the modulus of elasticity (MOE) of the adhesive. Since the MOE value of resorcinol-phenol-formaldehyde is higher than that of southern yellow pine, the glue lines in the poles essentially serve as reinforcing for the poles. This shows that the wood composite poles may benefit from being reinforced by thin layers of a high strength material in the pole structure.

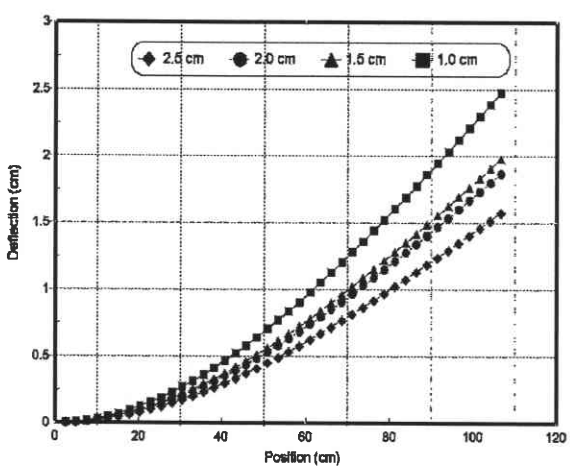

FIG. 6. Deflection of 12-sided small-scale composite poles predicted by a higher-order governing differential equation model.

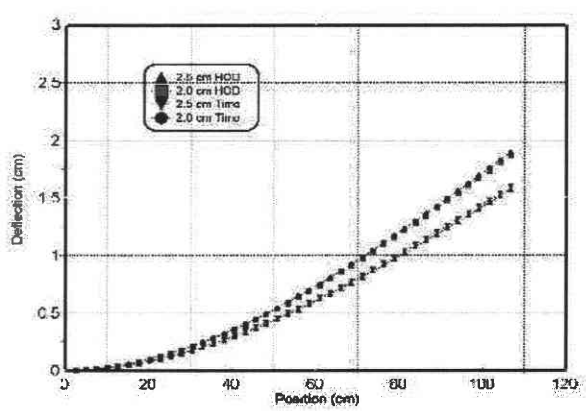

FIG. 7. Comparison of deflection of 12-sided small-scale composite poles predicted by a higher-order governing differential equation model and a simplified beam model.

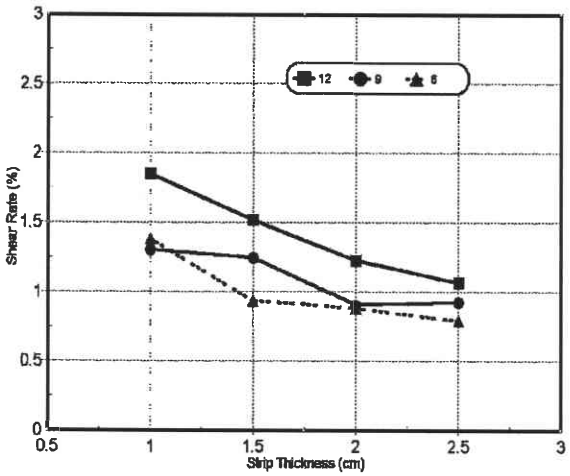

FIG. 8. Effects of strip thickness and number of strips on the shear deflection of small-scale composite poles.

Remarks on theoretical analysis procedures

A higher-order GDE model developed requires no correction factors that are required by the simplified theory and Timoshenko beam theory. Results of this study show that both the higher-order GDE model and simplified model agreed well with the experimental results.

Results also show that the simplified model was more accurate in predicting the deflection of small-scale composite poles than the higher-order GDE model. As shown in Eq. (36), the correction factor in the simplified model was approximated by a circular thick-shell cross-section. In practice, the calculation of the correction factor was not an easy task, especially when pole cross-section varies along the length, as in the case of a tapered pole. There was no such difficulty when using the higher-order GDE model. Since the dimension of the cross-section changes, k_8 and k_9 in Eq. (16) are no longer constants and can be calculated by integration. Thus, the higher-order GDE model has a wider application since variations in the cross-sections can be accounted for. Development of simplified theoretical models for tapered composite poles will be a good follow-up study.

The predicted deflection patterns for the small-scale composite poles are shown in Fig. 6. As expected, poles with thinner shell thickness are predicted to have a higher deflection than those with thicker shells for a given load.

SUMMARY AND CONCLUSIONS

A theoretical model was developed for wood laminated composite poles based on the principle of minimum potential energy. In addition to the transverse shear effects, the uniform gravity load and glue-line effects were included in the model. A simplified beam theory was also derived using the variational method and utilized to further validate the higher-order GDE model. These models and analyses will enable future investigation of composite poles with tapered forms and joined strips.

The theoretical model was developed based on Bernoulli-Euler theory and Timoshenko shear stress distribution theory. The governing equations were derived and solved, and the deformation function was obtained. The method provides solutions for the cantilever beam with a uniform load and/or concentrated load at the free end. Small-scale composite poles were fabricated and tested to validate the theoretical models. Strip thickness and number of strips (NOS) were chosen as experimental variables. The experimental results agreed very well with both theoretical models. The higher-order GDE model, though less accurate than the simplified model in this study, was found to be clearly more suitable for analyzing complex pole geometries.

Based on the results of this study, the following conclusions are made:

1. A higher-order governing differential equation model was developed and verified by the experimental results. The correlation of the higher-order governing differential equation model with the experimental results was good.
2. The higher-order governing differential equation model correlated well with the simplified beam model. However, the simplified model was more accurate than the higher-order GDE model in predicting the deflection of small-scale composite poles.

3. The higher-order GDE model was more suitable for analyzing complex pole geometries.
4. Deflection attributable to the glue layers accounted for about 4% of the total deflection of the composite poles.
5. Shear deflection accounted for 1 to 2% of total deflection.
6. Laminated composite poles may be reinforced by introducing a thin layer of a high strength material in the pole structure.

REFERENCES

BIBLIS, E. J. 1965. Shear deflection of wood beams. Forest Prod. J. 15(11):492–498.

BODIG, J, AND B. A. JAYNE. 1982. Mechanics of wood and wood composites. Van Nostrand Reinhold, New York, NY. 712 pp.

GRASHOF, F. 1878. Elastizitat und Festigkent. 2nd ed. Auflage der "Festigkeitslehre," Berlin, Germany.

KANT, T., AND A. GUPTA. 1988. A finite element model for a higher-order shear-deformable beam theory. J. Sound Vibr. 125(2):193–202.

KATHNELSON, A. N. 1996. Improved engineering theory for uniform beams. Acta Mech. 114:225–229.

RANKINE, W. J. M. 1895. Applied mechanics. 15th ed. Griffin and Co., London, England.

REHFIELD, L. W., AND P. L. N. MURTHY. 1982. Toward a new engineering theory of bending: fundamentals. AIAA Journal 20(5):693–699.

SHAMES, I. H., AND C. L. DYM. 1985. Energy and finite element methods in structural mechanics. Hemisphere Publishing Corporation, 757 pp.

TIMOSHENKO, S. P. 1921. On the correction for shear of the differential equation for transverse vibrations of prismatic bars. Philos. Mag. 41(6):744–746.

———. 1976. Strength of materials. Part I, 3rd ed., Robert E. Krieger Publishing Co., New York, NY.

VALISETTY, R. R. 1990. Refined bending theory for beams of circular cross section. J. Eng. Mech. 116(9):2072–2079.

WASHIZU, K. 1968. Variational methods in elasticity and plasticity. Pergamon Press. Oxford, New York, 349 pp.